Feature and Classification Analysis for Detection and Classification of Tongue Movements From Single-Trial Pre-Movement EEG

Rasmus L. Kæseler, Tim Warburg Johansson, Lotte N. S. Andreasen Struijk, and Mads Jochumsen

***Abstract*— Individuals with severe tetraplegia can benefit from brain-computer interfaces (BCIs). While most movement-related BCI systems focus on right/left hand and/or foot movements, very few studies have considered tongue movements to construct a multiclass BCI. The aim of this study was to decode four movement directions of the tongue (left, right, up, and down) from single-trial pre-movement EEG and provide a feature and classifier investigation. In offline analyses (from ten individuals without a disability) detection and classification were performed using temporal, spectral, entropy, and template features classified using either a linear discriminative analysis, support vector machine, random forest or multilayer perceptron classifiers. Besides the 4-class classification scenario, all possible 3-, and 2-class scenarios were tested to find the most discriminable movement type. The linear discriminant analysis achieved on average, higher classification accuracies for both movement detection and classification. The right- and down tongue movements provided the highest and lowest detection accuracy (95.3±4.3% and 91.7±4.8%), respectively. The 4-class classification achieved an accuracy of 62.6±7.2%, while the best 3-class classification (using left, right, and up movements) and 2-class classification (using left and right movements) achieved an accuracy of 75.6±8.4% and 87.7±8.0%, respectively. Using only a combination of the temporal and template feature groups provided further classification accuracy improvements. Presumably, this is because these feature groups utilize the movement-related cortical potentials, which are noticeably different on the left- versus right brain hemisphere for the different movements. This study shows that the cortical representation of the tongue is useful for extracting control signals for multi-class movement detection BCIs.**

Manuscript received September 21, 2021; revised January 23, 2022; accepted February 27, 2022. Date of publication March 15, 2022; date of current version March 22, 2022. This work was supported in part by the Independent Research Fund Denmark under Grant 8022-00234B and in part by VELUX FONDEN under Grant 22357. *(Lotte N. S. Andreasen Struijk and Mads Jochumsen contributed equally to this work.) (Corresponding author: Rasmus L. Kæseler.)*

This work involved human subjects or animals in its research. Approval of all ethical and experimental procedures and protocols was granted by the Local Ethical Committee of Region North Jutland under Application No. N-20130081.

Rasmus L. Kæseler and Lotte N. S. Andreasen Struijk are with the Center for Rehabilitation Robotics, Department of Health Science and Technology, Aalborg University, 9220 Aalborg, Denmark (e-mail: rlk@hst.aau.dk; naja@hst.aau.dk).

Tim Warburg Johansson and Mads Jochumsen are with the Department of Health Science and Technology, Aalborg University, 9220 Aalborg, Denmark (e-mail: tjohan16@student.aau.dk; mj@hst.aau.dk).

This article has supplementary downloadable material available at https://doi.org/10.1109/TNSRE.2022.3157959, provided by the authors.

Digital Object Identifier 10.1109/TNSRE.2022.3157959

***Index Terms*— Brain-computer interfaces, EEG, movement-related cortical potentials, tongue.**

I. Introduction

INDIVIDUALS with tetraplegia, such as individuals with a spinal cord injury (SCI), amyotrophic lateral sclerosis (ALS), or multiple sclerosis, are often dependent on caregivers for simple daily tasks, and the lack of functionality has been shown to cause depression and low quality of life [1]–[5].

Assistive technologies, such as an electric wheelchair or a robotic arm, can give individuals with tetraplegia independence and possibly improve their quality of life. However, controlling such technologies requires a very high-performing interface [6] with access to a high number of control commands with high input recognition and low latency; e.g., 14 control commands are required for manual control of a seven degrees of freedom robotic arm. This is a challenge to provide individuals with severe disabilities. Individuals with tetraplegia who still have motor functionality above the neck, such as individuals with SCI or early spinal-onset ALS, can use some control options such as lip-sip-suck control [7], [8], eye-tracking [9]–[11], or electrooculography (EOG) or facial electromyography (EMG) [12], or tongue control [13]–[20]. However, if the cranial nerves are also affected the individual may be in a locked-in state (LIS) and can then only use a brain-computer interface (BCI) as a control option. A BCI, measures and classifies brain activity to determine the user's control intent independently of any physical movement [21]. Electroencephalography (EEG) is popularly used to measure brain activity for BCI systems as it provides a decent signal quality with high temporal resolution while remaining non-invasive. The best performing BCI systems rely on stimuli (typically visual such as P300 [22], steady-state visually evoked potentials (SSVEP) [23] or code visually evoked potentials (C-VEP) [24] as they allow a high number of classes that can be detected with high accuracy. However, they require attention to the stimuli which may reduce the overall control of a robotic arm as the users have reduced attention to the robot. Furthermore, the stimuli might cause fatigue and/or require eye-gaze which some LIS patients do not have. As an alternative to stimuli-based BCI, Nam *et al.* utilized the glossokinetic potentials (GKP), which are elicited when the tip of the tongue makes contact with tissue inside the mouth [13], [18]–[20], to successfully control a robotic wheelchair through EEG measurements [18]. While

it showed a new control option, it requires physical tongue movements similar to other proposed tongue control interfaces that achieve a higher performance [16], [17], [25], [26]. Furthermore, individuals with LIS will require a different system as these individuals have limited to no tongue movement. For these individuals we consider BCI systems utilizing signals generated not only by performing a movement, but also by attempting and/or imagining one; specifically Movement-Related Cortical Potentials (MRCP), Event-Related Synchronization (ERS), and Event-Related Desynchronization (ERD) [27]–[29]. Most typically hand and foot movements have been investigated, and typically tongue movements are only included as a single class (such as the 4th class in a BCI using the left- and right hand, either of the feet, and the tongue as different classes) [30]–[32]. To implement more and/or alternative classes, studies have investigated the possibility of distinguishing between different movement types for a single muscle group, specifically different hand movements as the hand has a large cortical representation (compared with the foot) [33]–[35]. The muscle group of the tongue has a high cortical representation, as it exists on both the left- and right hemispheres (near lateral sulcus, at the far lateral positions of the primary motor cortex). Still, tongue movement types and classification of such have not yet been studied. Until now tongue movements have been treated as undesirable artifacts [36], or a single muscle group (class) [30], or with a focus on GKP [20]. In a feasibility study, we showed the possibility of classifying different tongue-movement types (left, right, up, and down movement) using only EEG signals generated before the actual movement [37].

In summary, there is a gap in the current literature on constructing a stimulus-independent multiclass BCI based on tongue movements that could be used for increasing the number of classes in a BCI for control of robots requiring a high number of control commands. Therefore, the aims of this study were to detect and classify four different tongue movement types using single-trial pre-movement EEG and perform a feature and classifier investigation of commonly used BCI techniques to create a reference point for future investgations regarding decoding of these novel (in a BCI context) movement types. Moreover, it was investigated what movement types to use if a 3- or 2-class system should be used instead of a 4-class system.

II. Methods

A. Participants

Ten individuals without a disability participants (8 men, 2 women, age 26.7±2.9 years) were recruited for this experiment. Before the experiment, the participants provided their written informed consent. All procedures were approved by the local ethical committee of Region North Jutland (N-20130081) and followed the Helsinki Declaration.

B. Experimental Setup

The experimental data were collected in collaboration with a master student as part of teaching activities at the Biomedical Engineering and Informatics education [38].

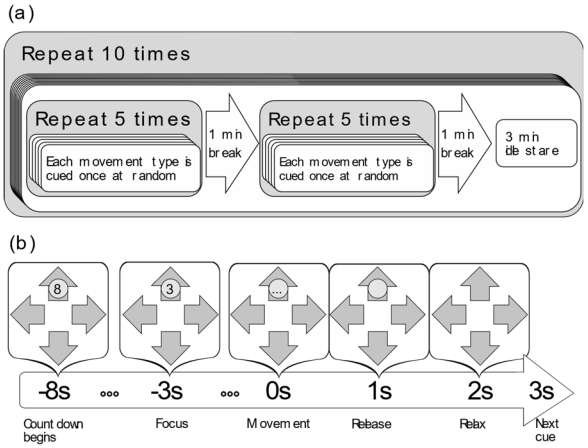

Fig. 1. Schematic overview of the experimental design. (a) The timing schedule for executing the cued movement, gathering idle EEG and having short breaks during the experiments. (b) The cueing presentation, exemplified with a "upwards" cue. Each movement type was cued a total of 100 times.

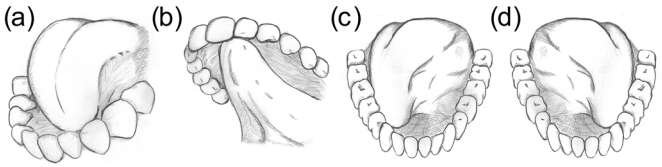

Fig. 2. Schematic overview of four types of tongue movements; (a) the downwards movement, (b) the upwards movement, (c) the right movement, and (d) the left movement.

The participants were seated in a comfortable chair in an electrically shielded room and were instructed to perform four different cued movement types of the tongue: left, right, up, and down. Fig. 1(a) illustrates the experimental design with the cue scheduling being illustrated in Fig. 1(b). Fig. 2 illustrates the four instructed tongue movements. The instructions to perform the movements were to touch the lower left or right hard palate or the floor of the mouth with the tip of the tongue when performing the left or right movements, respectively. For the up and down movements, the participants were asked to touch the front upper or lower teeth with the tip of the tongue, respectively.

The experiment was divided into 10 blocks; within each block, each movement type was cued 2×5 times distributed over two rounds with a 1-minute break in-between. The two rounds were followed by a 3-minute period during which idle activity was recorded and the participants were instructed to fixate on a point on a wall two meters away. The movements were visually cued and randomized by a custom-made Python script. The participants were presented with the movement type they were about to perform eight seconds before the movement onset. A counter was counting down from 8 seconds to 0 seconds, with 0 seconds being the instant where the participants should initiate the movement. After the initiation of the movement, they were asked to maintain the tongue in the desired position for two seconds. The participants were instructed to sit as still as possible and avoid blinking and activating facial muscles from three seconds before until

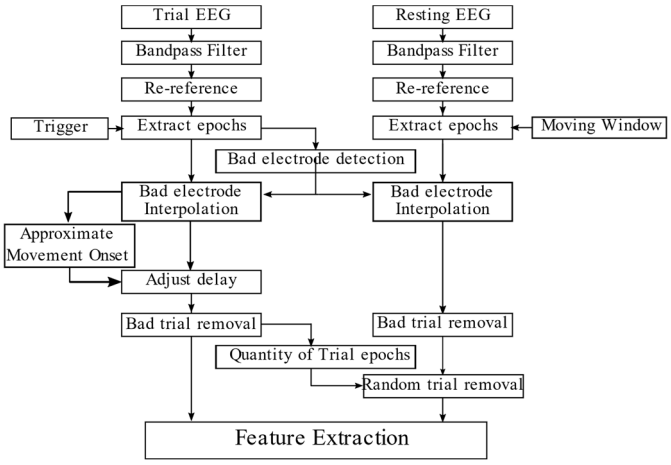

Fig. 3. Pre-processing of trial and resting EEG.

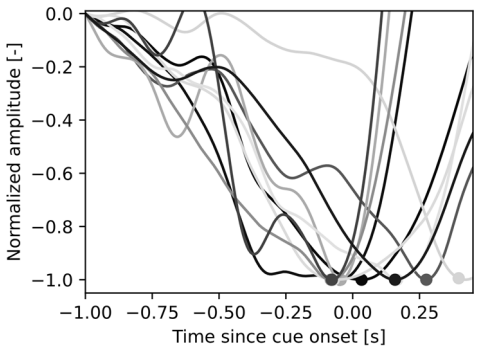

Fig. 4. The mean MRCP over all good trials and all electrodes in the FCx, Cx, CPx bands (in accordance with the 10-10 EEG electrode system), for each of the ten participants. The approximate movement onset was chosen at its minimum and marked with a dot. Cue-onset was set at 0s.

two seconds after the movement onset. At the beginning of each new trial, the custom-made python script sent a trigger to the EEG amplifier for synchronizing the EEG with the visual cues. In total, 400 tongue movements were performed: 100 movements up, down, left, and right.

C. Signal Acquisition and Pre-Processing

Continuous EEG data were recorded from 64 active electrodes according to the 10-10 EEG electrode system (g.GAMMAcap, G.Tec, Austria) and sampled at 512 Hz with a G.HIamp amplifier (G.Tec, Austria). The amplifier was connected to a PC running the g.Recorder software (G.Tec, Austria). The impedance of the electrodes was kept below 30 kΩ throughout the experiment. Electrodes were grounded and referenced to AFz and the left earlobe, respectively.

Fig. 3 shows the steps made to pre-process the raw EEG before the feature extraction. Initially, the continuous EEG was notch filtered at 50Hz to remove powerline noise using a 2^{nd} order Butterworth zero-phase filter, and then bandpass filtered between 0.1-45 Hz to remove the DC offset, drift, and the major components of potential EMG activity using a 4^{th} order Butterworth zero-phase bandpass filter. The electrodes were then re-referenced to the average between left- and right earlobe.

Bad electrodes and corrupted trials, in which noise and/or disturbances were excessively high, were identified by evaluating the peak-to-peak amplitude from two seconds before cue-onset until one second after. Electrodes that had a peak-to-peak amplitude above 150 μV in more than 25% of the trials were identified as bad; these were replaced by linear interpolation of the four nearest good electrodes as conducted in other literature [39] (Datafile S1 shows the removed electrodes for each subject).

A participant-specific delay between movement- and cue-onset was estimated and adjusted using an average MRCP measurement. The average MRCP was calculated for each participant, using data from one second before cue onset until one second after. First, all trials with a peak-to-peak amplitude above 150 μV in any electrode were identified as a bad trial and removed to avoid major undesirable artefacts (such as blinking or swallowing). Second, the average MRCP was estimated by averaging over electrodes in the primary motor cortex (FC7-FC8, C7-C8, and CP7-CP8) over all the included trials. The average movement-onset (aMO) was estimated as the peak negativity of the average MRCP; Fig. 4 shows the average MRCP for each participant, along with the aMO and the cue-onset. On average, the delay was 0.07 seconds for the ten subjects, with a maximum delay of 0.42 seconds (Datafile S1 shows the aMO for each subject). Trial epochs were then extracted from 2 seconds before aMO until aMO to avoid classifying EMG and GKP artefacts generated from actual movement. Resting epochs were extracted from the 10 blocks of 3-minute idle activity at random timestamps and sorted into separate folds (for 10-fold cross-validation) to ensure that overlapping windows would not be used for both training and test data. The maximum peak-to-peak amplitude over all electrodes was calculated for all epochs, and epochs with a maximum peak-to-peak amplitude above 150 μV were removed. Across the ten participants, an average of 7.07% of the trials was removed during this step (Datafile S1 shows the number of removed trials for each subject). Lastly, to balance the classification analyses, random resting epochs were removed until the number of resting epochs equaled that of the trial epochs.

D. Feature Extraction

To capture the pre-movement EEG activity, MRCP and SMR, four feature groups was were investigated as done in previous work [40]. Several feature types were extracted for each feature group to account for the inherent inter-subject variability and unexplored movement type.

A total of 50 feature types were extracted from each electrode channel individually; 25 feature types were extracted from a 2s-window while the remaining 25 were similarly extracted but from a 0.5s window, i.e., from either 2s or 0.5s until aMO. All features were standardized (subtracting the mean and scaling to unit variance) against the training data before being used for classification.

1) Temporal Features (T): A total of six temporal feature types were extracted from each window. The feature types were the mean value (1), the minimum peak (2), the maximum

peak (3), the peak-to-peak value (4), the slope (5), and the intersection (6) of a linear regression within the full and reduced window.

2) Template Features (X): A total of ten template feature types were extracted from each window. Four template signals were calculated for each of the cued movements, as the average of all training trials belonging to the respective cue. A fifth template signal was calculated as the average across all the training trials. Feature types were calculated as both the Pearson Correlation between the trial and the right- (1), up- (2), left- (3), down- (4)-, or combined movement template (5); and the maximum cross-correlation between the trial and the right- (6), up- (7), left- (8), down- (9)-, or combined movement template (10).

3) Spectral Features (S): A total of five spectral feature types were extracted from each window. Welch's power spectral density estimate was calculated using a Hann window with a 50% overlap of the segments. The mean power was calculated for the [0-4Hz] delta- (1), [4-8Hz] theta- (2), [8-13Hz] alpha/mu- (3), [13-30Hz] beta- (4), and [30-45Hz] gamma bands (5) for the full window and the reduced window.

4) Entropy Features (E): A total of four entropy feature types were extracted from each window. Approximate entropy, permutation entropy, sample entropy, and constrained entropy. An embedding dimension of $m = 2$ was used. The tolerance was calculated as 20% of the standard deviation of the epoch for all except the constrained entropy method, which instead used the 20% of the standard deviation of a "noise" epoch extracted from three seconds before aMO until the start of the extraction window.

E. Feature Reduction

To reduce the number of features used for the classification, two algorithms were used: (1) Sequential Forward Selection (SFS) [34] and (2) Principal component analysis (PCA).

1) Sequential Forward Selection: To utilize only useful features SFS was used on each feature group (temporal, template, spectral, and entropy) to estimate which of the feature types (i.e. mean value, minimum peak etc. for the temporal feature group) within the group provided a classification accuracy improvement. The algorithm has two steps: (1) ranking the feature types and (2) evaluating each feature type to determine if it should be saved for future classifications. To rank the feature types, the classification accuracy was estimated for each feature type within the investigated group. The feature types were then ranked from highest to lowest achieved accuracy; the highest ranked feature type was saved for classification of the test data. The lower ranked feature types were then sequentially evaluated (from highest to lowest rank) by estimating the classification accuracy (using the training data) when including both the feature type and the already saved feature types: if the accuracy improved, the investigated feature type was also saved for classification of the test data, otherwise it was excluded. For each feature type, classifier, and subject the percentage of folds where a feature type was included, for movement detection and classification is shown in Datafile S2 and S3, respectively.

2) Principal Component Analysis: PCA was used for each feature type to extract only the principal component of the investigated class over the electrodes. Using the training data, the principal components were calculated for each of the included feature types as the components which explained 99% of the variance over the electrodes. The principal components for all features were then concatenated and used for classification. The summation of the absolute principal component weights indicates which electrodes provide most important information for each movement type. The supplementary Fig. S1 show the absolute sum of weights, normalized and then averaged over all participants, for each feature type and movement type.

F. Classification

Four classifiers were compared in this study: A linear discriminative analysis (LDA), a support vector machine (SVM), a random forest classifier (RF), and a Multilayer Perception classifier (MLP). The classifiers available from the scikit-learn python library package were used [https://scikit-learn.org/stable/]. The LDA was implemented with an eigenvalue decomposition solver and automatic shrinkage using the Ledoit-Wolf lemma for the classifications. The SVM was implemented with a radial basis function kernel with a $C = 10.0$ and the reciprocal of the number of features as the kernel coefficient. The RF was implemented with 400 trees, using the Gini impurity as a quality measure for each split. The MLP was designed with one hidden layer with $2N + 1$ neurons, where N is the number of features included in the classification. 10-fold cross-validation was used to estimate the accuracy of the training data; classifiers were compared using the same folds. All classifications were made as one-versus-rest classification with a maximum probability as the decision function. The classification was separated into two analyses: (1) detection of tongue movement and (2) classification of the tongue movement type. In the detection of movements, all movement types were pooled as the same class and classified against the idle class in a 2-class classification scenario. To investigate the detection accuracy of the individual movement type, a 2-class classification between each movement type and the idle class was made for each of the four movement types. For the classification of movement type, each of the movement types was pooled as individual classes in a 4-class classifier. Also, a classification of all combinations of a 3-class and 2-class classification scenario was performed. All classes were balanced throughout the analysis.

G. Statistics

Statistical analysis was carried out using the IBM SPSS Statistics 27 software. For both detection and classification of movements, one-way repeated measures analysis of variance (rmANOVA) tests were used to investigate if there was a difference between the classification scenarios. For movement detection, there were four levels (Up, Right, Down, and Left). The classification accuracies for each classifier were pooled for the estimation of each movement type vs the idle activity. For movement classification, there were four and six levels for the

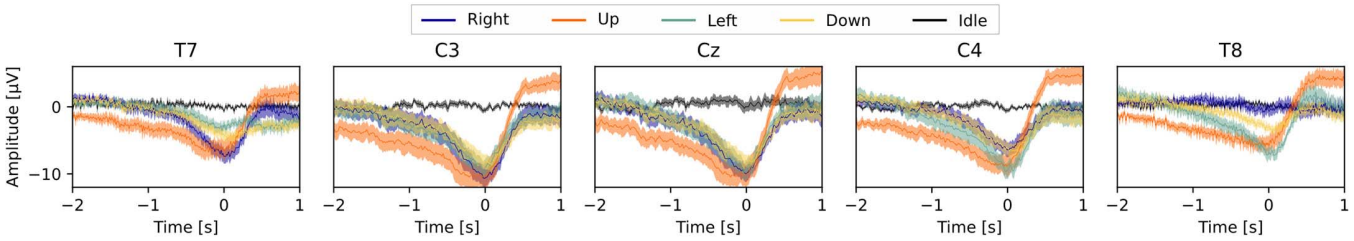

Fig. 5. Grand averages across participants of the MRCP during tongue movements with the approximate movement onset on t = 0s, here presented from five evenly spaced electrodes on the motor band: T7, C3, Cz, C4 and T8. The shaded area indicates the standard error.

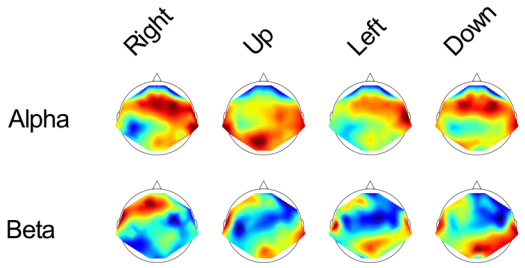

Fig. 6. Grand average topological plots of the Alpha [8]–[13] Hz and Beta [13]–[30] Hz bandpower at movement onset, for the four different movement types averaged across all subjects and all trials. The power was calculated as mean-square of the bandpass filtered signal, referenced to common average reference, from 0.5 seconds before until movement onset.

3-class and 2-class classification scenarios, respectively (using the possible combination of movements). The classification accuracies for each classifier were pooled for the estimation of each combination of movement types. Moreover, two rmANOVAs were performed to test if there was a difference between the classification methods for movement detection and classification. The analysis of the classification method was designed with four levels (LDA, SVM, RF, and MLP). The calculated accuracies were pooled from the accuracy estimations using all feature types. For movement detection, the accuracies were pooled for the estimation of idle versus each movement type and versus all movement types combined. For movement classification, the accuracies for each classification scenario were pooled. Significant tests were assumed when $p < 0.05$. Significant test statistics were followed up with post hoc analysis using Bonferroni correction.

III. Results

The grand average MRCP signal for each of the cued movements is shown in Fig. 5 for electrodes on the primary motor cortex. The left movement had a low MRCP peak negativity amplitude on T7 but the highest peak-negativity amplitude on T8 and vice-versa for the right movements. Downwards movements generally resulted in lower peak negativity amplitude, while upwards movements generally resulted in high peak negativity amplitudes.

A. Classification Methods and Scenarios

The classification accuracy was found for each classifier using all features. Different classification scenarios were investigated; a 4-class, 3-class, and 2-class scenario were investigated to provide information on the movement type classification. Table I shows the accuracies for the different combinations of movements using an LDA, SVM, or RF classifier. The movement detection and classification accuracies for each subject are included in Datafile S4 and Datafile S5, respectively.

TABLE I
Detection and Classification Accuracies for Different Scenarios

Type	Movement	LDA	SVM	RF	MLP
Detect	Right	**95.3±4.3**	90.0±4.3	93.9±4.7	92.5±5.0
	Up	93.0±5.1	89.0±5.0	91.6±5.5	91.3±4.9
	Left	94.3±4.5	89.5±3.2	94.1±4.1	92.0±4.2
	Down	91.7±4.8	85.9±4.3	90.6±4.9	88.3±4.7
	All	**93.7±4.0**	90.3±3.6	90.9±5.2	92.5±4.2
4-class	All	**62.6±7.2**	60.7±7.8	**62.6±6.7**	62.3±6.1
3-class	R/U/L	**75.6±8.4**	71.9±7.1	74.6±8.3	73.7±5.3
	R/U/D	69.9±6.9	66.8±6.4	70.7±5.1	69.7±5.0
	U/L/D	67.2±7.6	65.3±7.4	67.3±7.3	73.7±5.3
	R/L/D	71.7±9.5	66.9±10.9	70.5±9.3	69.7±5.0
2-class	R/U	86.2±5.8	81.3±6.8	85.4±5.8	84.1±4.9
	L/R	**87.7±8.0**	83.8±8.6	87.2±8.1	87.0±7.1
	R/D	80.8±8.8	75.3±9.7	80.9±8.9	80.1±7.9
	U/L	83.0±8.2	80.1±7.3	83.2±8.4	82.2±5.9
	U/D	78.7±9.9	77.8±8.6	79.0±11.2	78.5±9.0
	L/D	78.1±9.5	72.4±12.0	77.7±10.6	75.9±9.5

Accuracy of the different classifier types using a Linear Discriminative Analysis (LDA), Support Vector Machine (SVM), Random Forrest classifier (RF), or Multilayer Perceptron (MLP) classifier with all features. Abbreviations: Left movement (L), right movement (R), up movement (U), down movement (D). Highlighted with bold text the highest accuracy within each scenario

1) Movement Detection: From Table I it is observed that all classifiers achieved the highest mean accuracy when detecting right tongue movements (90-95%), while downwards movements achieved the lowest (86-92%). The LDA achieved the highest accuracy for all movement detection scenarios (92-95%), while SVM achieved the lowest (86-90%). A boxplot of the pooled accuracy estimations, concerning classifier type for the movement detection is shown in Fig. 7(a). The rmANOVA indicated a significant difference between the classifier-groups ($F(2.0, 99.6) = 48.54$, $p < 0.001$), and the post hoc analysis showed that LDA achieved significantly higher accuracies compared to the three other classifiers. Furthermore, the RF and MLP also performed significantly better than the SVM.

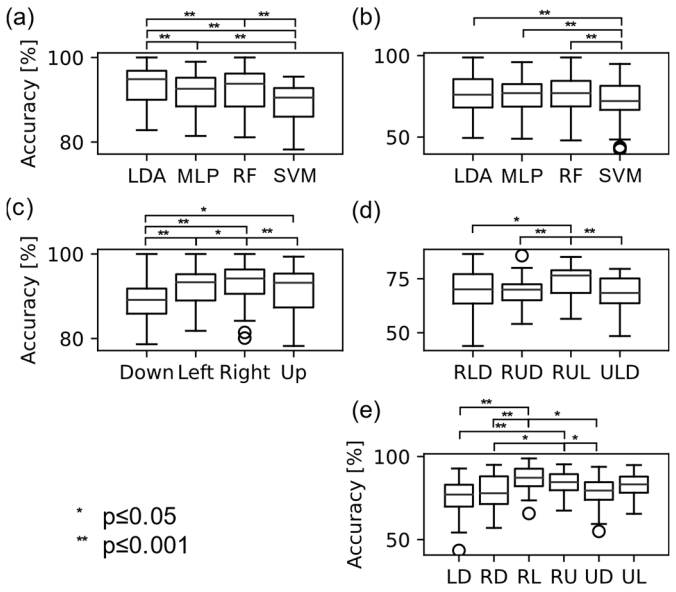

Fig. 7. The pooled accuracy estimations from all participants (N = 10) using all electrodes and all features. (a) Movement detection- and (b) movement classification accuracy estimations pooled for each classifier. (c) Movement detection accuracy pooled for each individual movement type. (d-e) Movement classification accuracy pooled for movement type composition in a 3-class and a 2-class classification scenario, respectively. Abbreviations: Left movement (L), right movement (R), up movement (U), down movement (D), linear discriminative analysis (LDA), support vector machine (SVM), random forest classifier (RF), and multilayer perceptron (MLP).

Fig. 7(b) shows boxplots of the pooled accuracy estimations concerning the individual movement types used for movement detection. The rmANOVA showed a significant difference between the groups for the movement detection of the individual movement types ($F(1.9, 74.8) = 14.93$, $p < 0.001$) with post hoc showing that the down movement had a significantly lower detection accuracy compared with both the left and right movement. The right movement type also achieved a significantly higher detection accuracy compared to the left movements.

2) Movement Classification: From Table I it is observed that the LDA and RF achieved the highest 4-class classification accuracy (63%) when using all four movement groups. With the 3-class and 2-class classifications, the LDA achieved the highest accuracies with the Right-Up-Left (76±8%) and the Right-Left (88±8%) scenarios. A boxplot of the pooled accuracy estimations concerning classifier type is shown in Fig. 7(c). The rmANOVA indicated a significant difference between the classifier-groups ($F(2.3,252.3) = 34.01$, $p < 0.001$) with the post hoc analysis showing that the SVM achieved significantly lower accuracies compared to all other classifiers.. Figure 7(d) and Fig. 7(e) show the combination of movement types for a 3-class and 2-class system, respectively. The rmANOVA showed a significant difference within both the 3-class classification scenarios ($F(2.4, 92.6) = 9.84$, $p < 0.001$) and 2-class classification scenarios ($F(2.3,87.7) = 10.65$, $p < 0.001$). For the 3-class movement classification, the post hoc analysis indicated that the Right-Up-Left classification scenario achieved a significantly higher accuracy compared all other scenarios. For the 2-class classification scenarios, the post hoc analysis showed that both the Right-Left and Right-Up classification scenarios achieved significantly higher accuracies compared to the Right-Down, Left-Down and Up-Down scenarios.

B. Feature Analysis

To analyse which combination of feature group would provide the highest accuracy, both the movement detection accuracy and movement classification accuracy were estimated using each of the 15 possible combinations of the four feature groups.

1) Movement Detection: Fig. 8(a) shows the estimated detection accuracy of all four movement types for each classifier. Datafile S6 includes the estimated detection accuracies for each individual subject. Using the LDA with all feature groups achieved the highest mean movement detection accuracy (94±4%) across all classifiers and feature types. The other classifiers also achieved the highest mean accuracy using all feature groups(90-93%).

The entropy feature group (E) achieved the lowest accuracy for all classifiers (78-80%). When using only one feature group, the temporal feature types (T) achieved the highest accuracy for all classifiers (87-89%).

2) Movement Classification: Fig. 8(b) shows the estimated classification accuracy for each 4-class classifier. Datafile S7 includes the estimated detection accuracies for each individual subject. Using the MLP classifier with the Temporal+Template (T+X) combination achieved the highest accuracy for movement classification (64±6%). The SVM also achieved the highest accuracy using this combination of feature groups (63±7), while the LDA and RF achieved the highest accuracy using the Temporal+Spectral+Template (T + S + X) combination (63±7% and 64±6%, respectively). The spectral and entropy features alone (S and E) and in combination (S+E) achieved much lower accuracies compared with all other combinations (25-33%across the four classifiers). When using only one feature group, SVM achieved the highest accuracy using the template feature group (61±7%), while LDA, RF, and MLP achieved the highest accuracy using the temporal feature group (62%).

IV. Discussion

In this study, it was shown that different tongue movement types could be detected with accuracies in the range of 92-95% with LDA which was significantly higher than the three other classifiers. The LDA also achieved the highest accuracies for classification of the different movement types, with an accuracy of 64%, 76%, and 88% for a 4, 3, and 2-class classification scenario, respectively. However, it was not shown to be significantly better than the RF or MLP for movement type classification.

A. Movement Detection

On average, a classification accuracy of 86-95% between pre-movement and idle activity was obtained. These findings

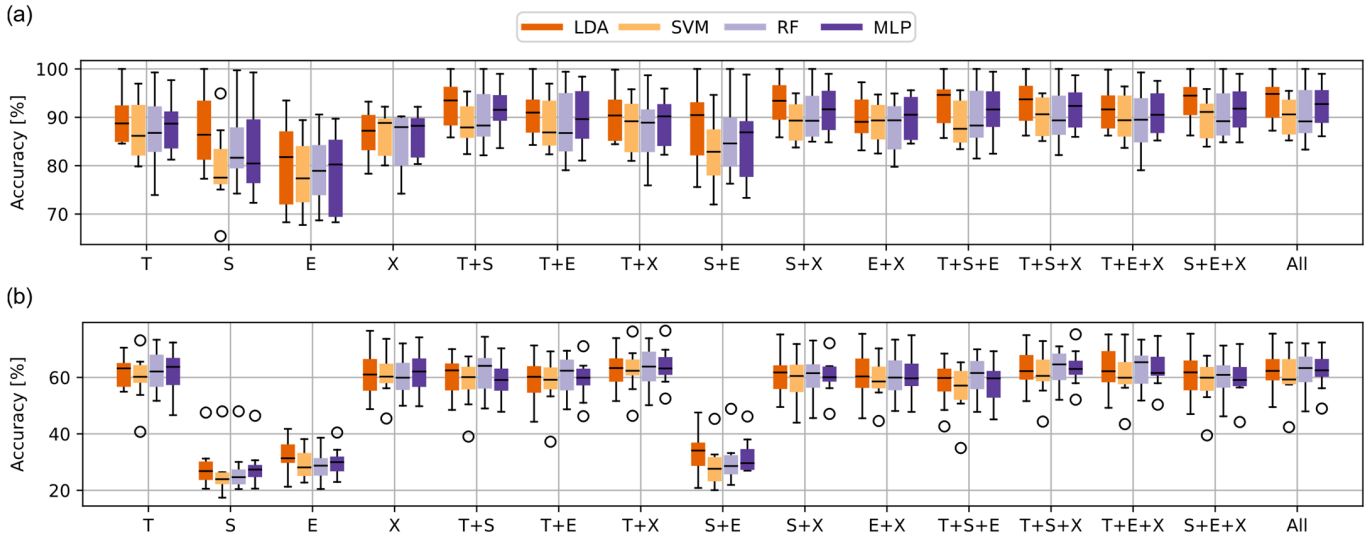

Fig. 8. Boxplots with a horizontal black line indicating the median for the movement detection accuracy (a) and movement classification accuracy (b) of all four movement types using combinations of either Temporal (T), Spectral (S), Entropy (E) and/or Template (X) features with wither an LDA, SVM, RF or MLP classifier.

are in line with the detection performance that has been reported in previous studies for the detection of upper and lower limb movements based on pre-movement EEG activity. It should be noted that different metrics, such as true positive rate and number of false-positive detections per minute, have been used and that some of the studies simulate an online BCI contrary to the simple 2-class classification paradigm in this study. The true positive rates and classification accuracies have been reported to be in the range of ∼70-95% for the lower limbs [40]–[49] and 75-95% for the upper limbs [34], [41], [50]–[54]. Different classifiers have been used in these studies, and LDA, SVM, RF, and MLP have all been reported to classify movement-related and idle activity well. In this study, the classification accuracies associated with each classifier were all significantly higher than the chance level (60% for 90 trials/class with a significance level of $\alpha = 5\%$) [55]. The LDA performed significantly better than the other classifiers which are beneficial for future online implementation of a BCI based on tongue movement-related activity due to the simplicity of the classifier. The different movement types were all detected well and there was no difference between the detection performance. This was also expected after observing the morphology of the MRCPs associated with the different tongue movements and the idle activity in Fig. 5, in which there was a clear difference in the peak of maximum negativity for the movement-related activity compared with the idle activity. The feature analysis revealed that all feature types could be used for detection of the tongue movement-related activity, but that the temporal, spectral, and template features were the most important ones, which is consistent with the existing literature within the detection of pre-movement EEG activity. The features types express some of the same discriminative information, but they also carry some complementary information which is indicated by higher detection performance when combining the feature types. This is also supported by the two neurophysiological phenomena movement-related cortical potentials and sensorimotor rhythms, which are different physiological signals associated with movement-related activity [27]. Combining temporal and spectral features has been conducted in several studies (see, e.g., [34], [49], [50]) as well as the combination of temporal, spectral, and template features for which good performance has been reported [56]. However, it should be noted that in this study there is a large standard deviation across the participants for the classification with the different feature combinations indicating that individualized features would be important for maximizing the detection performance.

B. Movement Classification

In this study, it was shown that different movement types of the same muscle group could be detected with relatively high classification accuracies. The decoding of different tongue movements shows similar classification accuracies as other studies in which movements from the same muscle group or limb have been performed. The classification accuracies for a 2-class system were in the range of 75-88% which is comparable to studies in which classification accuracies between 65-84% have been obtained for extracting different kinetic parameters[40], [41], [56]–[59], 72-79% for different hand movement types [34], [52], [60], 83% for gait direction [47], and 73-83% for different 2-class combinations of right hand, left hand, foot, or tongue movement [61]. With the 2-class scenarios, the Right-Left scenario achieved the highest mean accuracy across all classifiers. This is also indicated in Fig. 5 in which the peak of maximal negativity is smaller in T7 (left hemisphere) for left tongue movements and right tongue movements are smaller in T8 (right hemisphere). This indicates that tongue muscles can be divided into left and right subgroups acting similarly to left- and right-hand movements. For the 3-class classification scenarios, accuracies between 65-76% were obtained. In similar 3-class classification scenarios, 63-65% of hand movements [34], [62] and 60-78%

of lower limb movement [46], [47] were correctly classified. For the 4-class classification scenario, 64% were correctly classified with RF. Similar 4-class classification scenarios have reported accuracies in the range of 40-84% for extracting movement kinetics from hand and foot movements [40], [41], [56], [63], 76-% for extracting movement direction [64], [65], and 66% for different hand movement types [52]. As for the movement detection, the 2-, 3-, and 4-class classification accuracies were above chance level (60, 40, 30% for the 2-class, 3-class and 4-class scenario with 90 trials/class and a significance level of $\alpha = 5\%$) [55] for the four classifiers, but RF, MLP, and LDA performed better than SVM. For the feature analysis, it was shown that temporal and template features were the most important ones compared with spectral and entropy features and that these feature types did not provide much additional discriminative information to the classification.

Like the movement detection, there was a noticeable standard deviation across participants for the classification using different features which again indicates that individualizing features to the specific user would be important to maximize the BCI performance. Data-driven approaches without a-priori feature extraction could potentially improve the classification accuracies further. Convolutional Neural Network, Morphological Neural Networks, or Spiking Neuronal Network have previously been shown to improve classification performance [61], [63], [66].

C. Limitations

The focus of this paper was to detect and classify different movement types to be used for a multi-class BCI, but the offline analysis was performed with epochs were being extracted with a priori knowledge of when the movement occurred, and bad epochs were rejected from the analysis. However, the offline accuracies were high, so it is expected that good online BCI performance can be obtained although the online performance is most likely lower than the offline analysis. Also, the signal processing, feature extraction, and classification techniques used in this study can easily be transferred to an online BCI system. It could also be considered to use spatial filtering or other denoising techniques such as independent component analysis to make the detection of the movement intentions more robust [40], [42]. Moreover, 64 EEG channels were recorded and used in the analysis which is not practical for daily use in an online BCI. Therefore, the number of channels should be reduced. It has been shown that it is possible to use a single electrode for detecting movement intentions, but the decoding of kinetic profiles was moderate [56]. In another study, it was shown that the decoding of five different functional upper limb tasks could be decoded with an accuracy of 94% using 64 electrodes, but the accuracy dropped to 70% when using the ten best channels [67]. Thus, it would be possible to decrease the number of electrodes from 64 to a lower number while maintaining a decent BCI performance.

Another limitation of the study was that the data were collected from able-bodied participants contrary to the intended end-users who are individuals with severe motor impairments. However, in several studies it has been shown that movement-related activity can be detected and in some cases classify different movement parameters from people with motor impairments after, e.g., stroke [40], [56], cerebral palsy [48], spinal cord injury [68], and ALS [53], [54], [58]. Also, it is a possibility that individuals with spinal cord injury or ALS who have lost all voluntary muscle control below the neck may have a larger/more distinct cortical presentation of the tongue which potentially can lead to stronger control signals.

D. Implications

With the detection and classification of multiple tongue movement types, it would be possible to construct a multi-class BCI for control or communication applications. If manual control of a robotic arm with seven degrees of freedom should be obtained, 14 control commands must be available [69]. To obtain this it would be possible to combine a 2-, 3- or 4-class BCI system with a state machine [70] in which each state can be controlled with the classification of different tongue movements. As the cortical representation of the tongue is located near the ear, it could be a possibility to use minimalistic EEG headsets with few electrodes near the ear; thus, providing a hidden and/or aesthetic headset for users [71]. Also, it will be possible to avoid hair wash after each use if the electrodes are placed on the skin above/behind the ear which may be a desired feature for permanent BCI users.

V. Conclusion

In this study, it was shown that different tongue movements can be detected and classified from single-trial pre-movement EEG and potentially be used as an alternative approach to constructing a multi-class BCI based on movement-related brain activity. The detection and classification were possible with the different classifiers that were tested, but the best classifier was LDA. For movement detection, all tested feature types carried discriminative information, while the temporal and template feature types were the best for the classification of the different movement types. Until now, the detection and classification of different tongue movements from single-trial EEG have not been thoroughly investigated in the literature. In future studies, it should be investigated if decoding of these signals can be used as control signals in online BCI systems for controlling external devices and if such BCI systems can be operated by individuals with severe motor impairments.

References

[1] E. M. Holz, L. Botrel, T. Kaufmann, and A. Kübler, "Long-term independent brain-computer interface home use improves quality of life of a patient in the locked-in state: A case study," *Arch. Phys. Med. Rehabil.*, vol. 96, no. 3, pp. S16–S26, Mar. 2015, doi: 10.1016/j.apmr.2014.03.035.

[2] A. G. O. Ozanne, S. Strang, and L. I. Persson, "Quality of life, anxiety and depression in ALS patients and their next of kin," *J. Clin. Nursing*, vol. 20, nos. 1–2, pp. 283–291, Jan. 2011, doi: 10.1111/j.1365-2702.2010.03509.x.

[3] S. Paganoni *et al.*, "Functional decline is associated with hopelessness in amyotrophic lateral sclerosis (ALS)," *J. Neurol. Neurophysiol.*, vol. 8, no. 2, p. 423, 2017, doi: 10.4172/2155-9562.1000423.

[4] A. Gauthier *et al.*, "A longitudinal study on quality of life and depression in ALS patient–caregiver couples," *Neurology*, vol. 68, no. 12, pp. 923–926, Mar. 2007, doi: 10.1212/01.wnl.0000257093.53430.a8.

[5] H. Creemers, A. Beelen, H. Grupstra, F. Nollet, and L. H. van den Berg, "The provision of assistive devices and home adaptations to patients with ALS in The Netherlands: Patients' perspectives," *Amyotrophic Lateral Sclerosis Frontotemporal Degeneration*, vol. 15, nos. 5–6, pp. 420–425, Sep. 2014, doi: 10.3109/21678421.2014.920031.

[6] O. Tonet *et al.*, "Defining brain–machine interface applications by matching interface performance with device requirements," *J. Neurosci. Methods*, vol. 167, no. 1, pp. 91–104, Jan. 2008, doi: 10.1016/j.jneumeth.2007.03.015.

[7] M. A. Jose and R. de Deus Lopes, "Human–computer interface controlled by the lip," *IEEE J. Biomed. Health Informat.*, vol. 19, no. 1, pp. 302–308, Jan. 2015, doi: 10.1109/JBHI.2014.2305103.

[8] B. Aigner, V. David, M. Deinhofer, and C. Veigl, "FLipMouse: A flexible alternative input solution for people with severe motor restrictions," in *Proc. 7th Int. Conf. Softw. Develop. Technol. Enhancing Accessibility Fighting Info-Exclusion*, Dec. 2016, pp. 25–32, doi: 10.1145/3019943.3019948.

[9] P. Stawicki, F. Gembler, A. Rezeika, and I. Volosyak, "A novel hybrid mental spelling application based on eye tracking and SSVEP-based BCI," *Brain Sci.*, vol. 7, no. 4, p. 35, Apr. 2017, doi: 10.3390/brainsci7040035.

[10] A. Pasarica, R. G. Bozomitu, V. Cehan, and C. Rotariu, "Eye blinking detection to perform selection for an eye tracking system used in assistive technology," in *Proc. IEEE 22nd Int. Symp. for Design Technol. Electron. Packag. (SIITME)*, Oct. 2016, pp. 213–216, doi: 10.1109/SIITME.2016.7777280.

[11] H. Zeng *et al.*, "Semi-autonomous robotic arm reaching with hybrid gaze–brain machine interface," *Frontiers Neurorobot.*, vol. 13, pp. 1–17, Jan. 2020, doi: 10.3389/fnbot.2019.00111.

[12] F. D. P. Reynoso, P. A. N. Suarez, O. F. A. Sanchez, M. B. C. Yañez, E. V. Alvarado, and E. A. P. Flores, "A custom EOG-based HMI using neural network modeling to real-time for the trajectory tracking of a manipulator robot," *Frontiers Neurorobot.*, vol. 14, pp. 1–23, Sep. 2020, Art. no. 578834, doi: 10.3389/fnbot.2020.578834.

[13] M. Mace, R. Vaidyanathan, S. Wang, and L. Gupta, "Tongue in cheek: A novel concept in assistive human machine interface," *J. Assistive Technol.*, vol. 3, no. 3, pp. 14–26, Sep. 2009, doi: 10.1108/17549450200900020.

[14] M. Ghovanloo, "Tongue operated assistive technologies," in *Proc. 29th Annu. Int. Conf. IEEE Eng. Med. Biol. Soc.*, Aug. 2007, pp. 4376–4379, doi: 10.1109/IEMBS.2007.4353307.

[15] X. Huo and M. Ghovanloo, "Evaluation of a wireless wearable tongue-computer interface by individuals with high-level spinal cord injuries," *J. Neural Eng.*, vol. 7, no. 2, p. 26008, Apr. 2010, doi: 10.1088/1741-2560/7/2/026008.

[16] L. N. S. A. Struijk, L. L. Egsgaard, R. Lontis, M. Gaihede, and B. Bentsen, "Wireless intraoral tongue control of an assistive robotic arm for individuals with tetraplegia," *J. NeuroEng. Rehabil.*, vol. 14, no. 1, p. 110, Dec. 2017, doi: 10.1186/s12984-017-0330-2.

[17] M. Mohammadi, H. Knoche, M. Gaihede, B. Bentsen, and L. N. S. A. Struijk, "A high-resolution tongue-based joystick to enable robot control for individuals with severe disabilities," in *Proc. IEEE 16th Int. Conf. Rehabil. Robot. (ICORR)*, Jun. 2019, pp. 1043–1048, doi: 10.1109/ICORR.2019.8779434.

[18] Y. Nam, Q. Zhao, A. Cichocki, and S. Choi, "Tongue-rudder: A glossokinetic-potential-based tongue–machine interface," *IEEE Trans. Biomed. Eng.*, vol. 59, no. 1, pp. 290–299, Jan. 2012, doi: 10.1109/TBME.2011.2174058.

[19] Y. Nam, B. Koo, A. Cichocki, and S. Choi, "Glossokinetic potentials for a tongue-machine interface: How can we trace tongue movements with electrodes?" *IEEE Syst. Man, Cybern. Mag.*, vol. 2, no. 1, pp. 6–13, Jan. 2016, doi: 10.1109/MSMC.2015.2490674.

[20] K. Görür, M. R. Bozkurt, M. S. Bascil, and F. Temurtas, "Tongue-operated biosignal over EEG and processing with decision tree and kNN," *Academic Platform J. Eng. Sci.*, vol. 9, no. 1, pp. 112–125, Jan. 2021, doi: 10.21541/apjes.583049.

[21] U. Chaudhary, N. Mrachacz-Kersting, and N. Birbaumer, "Neuropsychological and neurophysiological aspects of brain-computer-interface (BCI) control in paralysis," *J. Physiol.*, vol. 599, no. 9, pp. 2351–2359, May 2021, doi: 10.1113/JP278775.

[22] L. M. McCane *et al.*, "Brain-computer interface (BCI) evaluation in people with amyotrophic lateral sclerosis," *Amyotrophic Lateral Sclerosis Frontotemporal Degeneration*, vol. 15, nos. 3–4, pp. 207–215, Jun. 2014, doi: 10.3109/21678421.2013.865750.

[23] X. Chen, B. Zhao, Y. Wang, and X. Gao, "Combination of high-frequency SSVEP-based BCI and computer vision for controlling a robotic arm," *J. Neural Eng.*, vol. 16, no. 2, Apr. 2019, Art. no. 026012, doi: 10.1088/1741-2552/aaf594.

[24] B. Wittevrongel, E. Van Wolputte, and M. M. Van Hulle, "Code-modulated visual evoked potentials using fast stimulus presentation and spatiotemporal beamformer decoding," *Sci. Rep.*, vol. 7, p. 15037, Dec. 2017, doi: 10.1038/s41598-017-15373-x.

[25] L. N. S. A. Struijk *et al.*, "Development and functional demonstration of a wireless intraoral inductive tongue computer interface for severely disabled persons," *Disab. Rehabil., Assistive Technol.*, vol. 12, no. 6, pp. 631–640, Aug. 2017, doi: 10.1080/17483107.2016.1217084.

[26] L. N. S. A. Struijk, "An inductive tongue computer interface for control of computers and assistive devices," *IEEE Trans. Biomed. Eng.*, vol. 53, no. 12, pp. 2594–2597, Dec. 2006, doi: 10.1109/TBME.2006.880871.

[27] H. Shibasaki and M. Hallett, "What is the bereitschaftspotential?" *Clin. Neurophysiol.*, vol. 117, no. 11, pp. 2341–2356, Nov. 2006, doi: 10.1016/j.clinph.2006.04.025.

[28] G. Pfurtscheller, "Functional brain imaging based on ERD/ERS," *Vis. Res.*, vol. 41, nos. 10–11, pp. 1257–1260, May 2001, doi: 10.1016/S0042-6989(00)00235-2.

[29] G. Pfurtscheller and F. H. L. da Silva, "Event-related EEG/MEG synchronization and desynchronization: Basic principles," *Clin. Neurophysiol.*, vol. 110, no. 11, pp. 1842–1857, Nov. 1999, doi: 10.1016/S1388-2457(99)00141-8.

[30] V. Morash, O. Bai, S. Furlani, P. Lin, and M. Hallett, "Classifying EEG signals preceding right hand, left hand, tongue, and right foot movements and motor imageries," *Clin. Neurophysiol.*, vol. 119, no. 11, pp. 2570–2578, Nov. 2008, doi: 10.1016/j.clinph.2008.08.013.

[31] G. Pfurtscheller, C. Brunner, A. Schlögl, and F. H. L. da Silva, "Mu rhythm (de)synchronization and EEG single-trial classification of different motor imagery tasks," *NeuroImage*, vol. 31, no. 1, pp. 153–159, May 2006, doi: 10.1016/j.neuroimage.2005.12.003.

[32] C. Liu, H. Wang, and Z. Lu, "EEG classification for multi-class motor imagery BCI," in *Proc. 25th Chin. Control Decis. Conf. (CCDC)*, May 2013, pp. 4450–4453, doi: 10.1109/CCDC.2013.6561736.

[33] K. Liao, R. Xiao, J. Gonzalez, and L. Ding, "Decoding individual finger movements from one hand using human EEG signals," *PLoS ONE*, vol. 9, no. 1, Jan. 2014, Art. no. e85192, doi: 10.1371/journal.pone.0085192.

[34] M. Jochumsen, I. K. Niazi, K. Dremstrup, and E. N. Kamavuako, "Detecting and classifying three different hand movement types through electroencephalography recordings for neurorehabilitation," *Med. Biol. Eng. Comput.*, vol. 54, no. 10, pp. 1491–1501, Oct. 2016, doi: 10.1007/s11517-015-1421-5.

[35] X. Yong and C. Menon, "EEG classification of different imaginary movements within the same limb," *PLoS ONE*, vol. 10, no. 4, Apr. 2015, Art. no. e0121896, doi: 10.1371/journal.pone.0121896.

[36] S. Vanhatalo, J. Voipio, A. Dewaraja, M. Holmes, and J. Miller, "Topography and elimination of slow EEG responses related to tongue movements," *NeuroImage*, vol. 20, no. 2, pp. 1419–1423, Oct. 2003, doi: 10.1016/S1053-8119(03)00392-6.

[37] R. L. Kaseler, L. N. S. Andreasen Struijk, and M. Jochumsen, "Detection and classification of tongue movements from single-trial EEG," in *Proc. IEEE 20th Int. Conf. Bioinf. Bioengineering (BIBE)*, Oct. 2020, pp. 376–379, doi: 10.1109/BIBE50027.2020.00068.

[38] T. W. Johansson. (2020). *Two-Class Classification of Tongue Movement in BCI for People With ALS*. Aalborg, Denmark. [Online]. Available: https://projekter.aau.dk/projekter/da/studentthesis/twoclass-classification-of-tongue-movement-in-bci-for-people-with-als(ad261fc6-ab94-4ce6-b939-06ac8092d7bc).html

[39] V. Mondini, R. J. Kobler, A. I. Sburlea, and G. R. Müller-Putz, "Continuous low-frequency EEG decoding of arm movement for closed-loop, natural control of a robotic arm," *J. Neural Eng.*, vol. 17, no. 4, Aug. 2020, Art. no. 046031, doi: 10.1088/1741-2552/aba6f7.

[40] M. Jochumsen, I. K. Niazi, N. Mrachacz-Kersting, N. Jiang, D. Farina, and K. Dremstrup, "Comparison of spatial filters and features for the detection and classification of movement-related cortical potentials in healthy individuals and stroke patients," *J. Neural Eng.*, vol. 12, no. 5, Oct. 2015, Art. no. 056003, doi: 10.1088/1741-2560/12/5/056003.

[41] M. Jochumsen, I. K. Niazi, N. Mrachacz-Kersting, D. Farina, and K. Dremstrup, "Detection and classification of movement-related cortical potentials associated with task force and speed," *J. Neural Eng.*, vol. 10, no. 5, Oct. 2013, Art. no. 056015, doi: 10.1088/1741-2560/10/5/056015.

[42] N. Jiang, L. Gizzi, N. Mrachacz-Kersting, K. Dremstrup, and D. Farina, "A brain–computer interface for single-trial detection of gait initiation from movement related cortical potentials," *Clin. Neurophysiol.*, vol. 126, no. 1, pp. 154–159, Jan. 2015, doi: 10.1016/j.clinph.2014.05.003.

[43] R. Xu, R. Xu, N. Jiang, C. Lin, N. Mrachacz-Kersting, K. Dremstrup, and D. Farina, "Enhanced low-latency detection of motor intention from EEG for closed-Loop brain-computer interface applications," *IEEE Trans. Biomed. Eng.*, vol. 61, no. 2, pp. 288–296, Feb. 2014, doi: 10.1109/TBME.2013.2294203.

[44] I. K. Niazi, N. Jiang, O. Tiberghien, J. F. Nielsen, K. Dremstrup, and D. Farina, "Detection of movement intention from single-trial movement-related cortical potentials," *J. Neural Eng.*, vol. 8, no. 6, Oct. 2011, Art. no. 066009, doi: 10.1088/1741-2560/8/6/066009.

[45] A. I. Sburlea, L. Montesano, and J. Minguez, "Continuous detection of the self-initiated walking pre-movement state from EEG correlates without session-to-session recalibration," *J. Neural Eng.*, vol. 12, no. 3, Jun. 2015, Art. no. 036007, doi: 10.1088/1741-2560/12/3/036007.

[46] T. C. Bulea, S. Prasad, A. Kilicarslan, and J. L. Contreras-Vidal, "Sitting and standing intention can be decoded from scalp EEG recorded prior to movement execution," *Frontiers Neurosci.*, vol. 8, no. 376, pp. 1–19, 2014, doi: 10.3389/fnins.2014.00376.

[47] P. D. Velu and V. R. de Sa, "Single-trial classification of gait and point movement preparation from human EEG," *Frontiers Neurosci.*, vol. 7, pp. 1–11, 2013, doi: 10.3389/fnins.2013.00084.

[48] M. Jochumsen, M. Shafique, A. Hassan, and I. K. Niazi, "Movement intention detection in adolescents with cerebral palsy from single-trial EEG," *J. Neural Eng.*, vol. 15, no. 6, Dec. 2018, Art. no. 066030, doi: 10.1088/1741-2552/aae4b8.

[49] E. N. Kamavuako, M. Jochumsen, I. K. Niazi, and K. Dremstrup, "Comparison of features for movement prediction from single-trial movement-related cortical potentials in healthy subjects and stroke patients," *Comput. Intell. Neurosci.*, vol. 2015, pp. 1–8, Oct. 2015, doi: 10.1155/2015/858015.

[50] J. Ibáñez *et al.*, "Detection of the onset of upper-limb movements based on the combined analysis of changes in the sensorimotor rhythms and slow cortical potentials," *J. Neural Eng.*, vol. 11, no. 5, Oct. 2014, Art. no. 056009, doi: 10.1088/1741-2560/11/5/056009.

[51] E. Lew, "Detection of self-paced reaching movement intention from EEG signals," *Frontiers Neuroeng.*, vol. 5, pp. 1–17, Jul. 2012, doi: 10.3389/fneng.2012.00013.

[52] A. Schwarz, P. Ofner, J. Pereira, A. I. Sburlea, and G. R. Müller-Putz, "Decoding natural reach-and-grasp actions from human EEG," *J. Neural Eng.*, vol. 15, no. 1, Feb. 2018, Art. no. 016005, doi: 10.1088/1741-2552/aa8911.

[53] A. M. Savić, S. Aliakbaryhosseinabadi, J. U. Blicher, D. Farina, N. Mrachacz-Kersting, and S. Došen, "Online control of an assistive active glove by slow cortical signals in patients with amyotrophic lateral sclerosis," *J. Neural Eng.*, vol. 18, no. 4, Aug. 2021, Art. no. 046085, doi: 10.1088/1741-2552/ac0488.

[54] S. Aliakbaryhosseinabadi, S. Dosen, A. Savic, J. Blicher, D. Farina, and N. Mrachacz-Kersting, "Participant-specific classifier tuning increases the performance of hand movement detection from EEG in patients with amyotrophic lateral sclerosis," *J. Neural Eng.*, vol. 18, no. 1, pp. 119–123, Jul. 2021, doi: 10.1088/1741-2552/ac15e3.

[55] G. R. Müller-putz, R. Scherer, C. Brunner, R. Leeb, and G. Pfurtscheller, "Better than random: A closer look on BCI results," *Int. J. Bioelectromagn.*, vol. 10, no. 1, pp. 52–55, 2008.

[56] M. Jochumsen, I. K. Niazi, D. Taylor, D. Farina, and K. Dremstrup, "Detecting and classifying movement-related cortical potentials associated with hand movements in healthy subjects and stroke patients from single-electrode, single-trial EEG," *J. Neural Eng.*, vol. 12, no. 5, Oct. 2015, Art. no. 056013, doi: 10.1088/1741-2560/12/5/056013.

[57] Y. Gu, O. F. do Nascimento, M.-F. Lucas, and D. Farina, "Identification of task parameters from movement-related cortical potentials," *Med. Biol. Eng. Comput.*, vol. 47, no. 12, pp. 1257–1264, Dec. 2009, doi: 10.1007/s11517-009-0523-3.

[58] Y. Gu, "Off line identification of imagined speed of wrist movements in paralyzed ALS patients from single-trial EEG," *Frontiers Neurosci.*, vol. 3, pp. 1–7, Aug. 2009, doi: 10.3389/neuro.20.003.2009.

[59] O. F. do Nascimento and D. Farina, "Movement-related cortical potentials allow discrimination of rate of torque development in imaginary isometric plantar flexion," *IEEE Trans. Biomed. Eng.*, vol. 55, no. 11, pp. 2675–2678, Nov. 2008, doi: 10.1109/TBME.2008.2001139.

[60] Y. Gu, K. Dremstrup, and D. Farina, "Single-trial discrimination of type and speed of wrist movements from EEG recordings," *Clin. Neurophysiol.*, vol. 120, no. 8, pp. 1596–1600, Aug. 2009, doi: 10.1016/j.clinph.2009.05.006.

[61] C. D. Virgilio G., J. H. Sossa A., J. M. Antelis, and L. E. Falcón, "Spiking neural networks applied to the classification of motor tasks in EEG signals," *Neural Netw.*, vol. 122, pp. 130–143, Feb. 2020, doi: 10.1016/j.neunet.2019.09.037.

[62] A. Schwarz, M. K. Höller, J. Pereira, P. Ofner, and G. R. Müller-Putz, "Decoding hand movements from human EEG to control a robotic arm in a simulation environment," *J. Neural Eng.*, vol. 17, no. 3, May 2020, Art. no. 036010, doi: 10.1088/1741-2552/ab882e.

[63] R. Gatti, Y. Atum, L. Schiaffino, M. Jochumsen, and J. B. Manresa, "Decoding kinetic features of hand motor preparation from single-trial EEG using convolutional neural networks," *Eur. J. Neurosci.*, vol. 53, no. 2, pp. 556–570, Jan. 2021, doi: 10.1111/ejn.14936.

[64] N. Robinson, C. Guan, A. P. Vinod, K. K. Ang, and K. P. Tee, "Multi-class EEG classification of voluntary hand movement directions," *J. Neural Eng.*, vol. 10, no. 5, Oct. 2013, Art. no. 056018, doi: 10.1088/1741-2560/10/5/056018.

[65] E. Y. L. Lew, R. Chavarriaga, S. Silvoni, and J. D. R. Millán, "Single trial prediction of self-paced reaching directions from EEG signals," *Frontiers Neurosci.*, vol. 8, pp. 1–13, Aug. 2014, doi: 10.3389/fnins.2014.00222.

[66] J. M. Antelis, B. Gudiño-Mendoza, L. E. Falcón, G. Sanchez-Ante, and H. Sossa, "Dendrite morphological neural networks for motor task recognition from electroencephalographic signals," *Biomed. Signal Process. Control*, vol. 44, pp. 12–24, Jul. 2018, doi: 10.1016/j.bspc.2018.03.010.

[67] M. Mohseni, V. Shalchyan, M. Jochumsen, and I. K. Niazi, "Upper limb complex movements decoding from pre-movement EEG signals using wavelet common spatial patterns," *Comput. Methods Programs Biomed.*, vol. 183, Jan. 2020, Art. no. 105076, doi: 10.1016/j.cmpb.2019.105076.

[68] E. López-Larraz, L. Montesano, Á. Gil-Agudo, and J. Minguez, "Continuous decoding of movement intention of upper limb self-initiated analytic movements from pre-movement EEG correlates," *J. Neuroeng. Rehabil.*, vol. 11, no. 1, pp. 1–15, 2014, doi: 10.1186/1743-0003-11-153.

[69] R. L. Kaseler, K. Leerskov, L. N. S. A. Struijk, K. Dremstrup, and M. Jochumsen, "Designing a brain computer interface for control of an assistive robotic manipulator using steady state visually evoked potentials," in *Proc. IEEE 16th Int. Conf. Rehabil. Robot. (ICORR)*, Jun. 2019, pp. 1067–1072, doi: 10.1109/ICORR.2019.8779376.

[70] R. Xu *et al.*, "Continuous 2D control via state-machine triggered by endogenous sensory discrimination and a fast brain switch," *J. Neural Eng.*, vol. 16, no. 5, Jul. 2019, Art. no. 056001, doi: 10.1088/1741-2552/ab20e5.

[71] M. Jochumsen, H. Knoche, P. Kidmose, T. W. Kjæ, and B. I. Dinesen, "Evaluation of EEG headset mounting for brain-computer interface-based stroke rehabilitation by patients, therapists, and relatives," *Frontiers Hum. Neurosci.*, vol. 14, pp. 1–10, Feb. 2020, doi: 10.3389/fnhum.2020.00013.